Supplementary Information for:

Wang et al, "Solution structure and functional analysis of the influenza B proton channel"

Supplementary Methods

Sample preparation

For structural studies of membrane proteins, establishing a suitable sample system has always been a major challenge. We have screened the intact full-length BM2 in many phosphocholine-based and sugar-based detergents as well as lyso lipids, but none yielded workable NMR spectra. To enable structural study, we established two NMR systems corresponding to two separate functional domains of the BM2 protein. For the channel region, we found that a construct encompassing residues 1-33 [BM2(1-33)] moves as a homogenous tetramer in SDS-PAGE without any chemical crosslinking when it is reconstituted in DHPC (dihexonyl-phosphocholine) micelles at pH 7.5 (Supplementary Fig. 10a). Under this condition, the sample also yields good ^{1}H-^{15}N and ^{1}H-^{13}C correlation spectra (Supplementary Fig. 10b&c). We also confirmed the function of this construct using liposomal proton flux assay. When reconstituted into liposomes made from *E.coli* lipid extract, BM2(1-33) shows specific proton conductance and that the conductance is completely insensitive to 50 M of rimantadine (Supplementary Fig. 3). The final buffer used for NMR measurement of BM2(1-33) contains ~300 mM DHPC, 15 mM βME and 40 mM sodium phosphate (pH 7.5).

For structural study of the C-terminal, water-exposed region of BM2, we identified a construct, BM2(26-109), which includes the entire predicted extramembrane region (residues 44-109) as well as six N-terminal residues that overlap with BM2(1-33). The purpose of including residues 27 – 43 was to provide structural information that potentially allow us to model the full length BM2 structure relative to a presumed lipid bilayer. BM2(26-109) is not soluble in water due the presence of hydrophobic residues from the TM domain and the membrane anchoring region that connects the TM and the cytoplasmic domains, but becomes soluble when it is bound to LMPG (1-Myristoyl-2-Hydroxy-sn-Glycero-3-[Phospho- rac-(1-glycerol)]) detergent micelles. SDS-PAGE of BM2(26-109) in LMPG without boiling shows that the majority of the protein runs as a tetramer in SDS (Supplementary Fig. 12a). NMR spectra show a single set of backbone and sidechain resonances, indicating a homogenous population of tetramers (Supplementary Fig. 12b&c). The final buffer used for NMR measurement of BM2(26-109) contains ~150 mM LMPG, 25 mM NaCl and 25 mM Tris buffer (pH 6.8).

Liposomal H+ flux assay

Nature Structural & Molecular Biology: doi:10.1038/nsmb.1707

An activity assay for BM2 channels was established based on works from the Schroeder, Miller and Busath labs (Schroeder et al., 1994; Nguitragool & Miller, 2006; Moffat et al., 2008). BM2(1-33) channels were reconstituted into liposomes by mixing 10 mg of *E. coli* polar lipid extract (Avanti Polar Lipids), 2.5 or 5 nmols of BM2(1-33) peptide, and 0.2 nmol of the potassium ionophore valinomycin in 1.1 mL of a 2:1 mixture of chloroform and methanol. The solution was dried down to thin films. Liposomes were then formed by resuspending the thin films in strongly-buffered internal liposome buffer (50 mM phosphate, 50 mM citrate, 122 mM KCl, 122 mM NaCl, 0.01% NaN_3, pH 7.7), and extruding 21 times through 0.2 μM polycarbonate membranes. The external buffer was exchanged by running 750 μL of the liposome solution over a PD-10 column (GE Health Sciences) pre-equilibrated with weakly-buffered external vesicle buffer (2 mM phosphate, 2 mM citrate, 122 mM KCl, 122 mM NaCl, 0.01% NaN_3, pH 7.8). Final eluted volume was 1.5 mL, containing 5 mg/mL lipid, 1.5 or 3 μM M2 peptide, and 0.1 μM valinomycin. From this, we estimate that there are ~15 or 30 channels per liposome, 50% of which, it is assumed, have the correct orientation to conduct protons into the liposome. Initial pH inside and outside of liposomes was identical. Protein-mediated conductance of protons from the bath into the liposomes was initiated lowering the external pH to 6.05-6.10 by addition of 3.5 μL of 1 M HCl with continuous rapid mixing. Proton flux was monitored as an increase in pH of the external bath with a pH micro-electrode (InLab). Reported flux rates were taken as the average rate observed over the period from 15 to 30 seconds after the addition of HCl. The assay was terminated by the addition of 5 μM of the proton ionophore carbonyl cyanide m-chlorophenylhydrazone (FCCP). To assay channel inhibition, rimantadine was added from concentrated stock solutions in anhydrous ethanol (Sigma) five minutes before initiation of proton flux. No change in pH upon addition of ethanol without rimantadine was observed. The effect of buffering from citrate, phosphate, rimantadine, and lipids was evaluated by addition of 5 μL of 50 mM HCl. Since the proton fluxes are taken as the initial change in pH, a correction factor was required to account for the increased buffering capacity of the solution after the system was uncoupled by FCCP. The excess buffering from the uncoupled liposome interiors was determined in a series of peptide-free controls containing 4.7, 5.0, or 5.3 mg/mL of lipid by adding 5 μL of 50 mM HCl before and after addition of FCCP.

NMR spectroscopy

NMR data analyses

Data processing and spectra analyses were done in NMRPipe [1] and CARA [2]. The program TALOS [3] was used to predict backbone dihedral angles from characteristic chemical shifts. Fitting of residual dipolar couplings (RDCs) to structures was done by singular value decomposition (SVD) [4], using the program

PALES [5].

Assignment of backbone and sidechain resonances

Sequence specific assignment of backbone $^{1}H^{N}$, ^{15}N, $^{13}C^{\alpha}$, $^{13}C^{\beta}$, and $^{13}C'$ chemical shifts were accomplished using the TROSY versions of the HNCA, HN(CO)CA, HNCACB, HN(CO)CACB, HN(CA)CO, and HNCO experiments [6,7] on ^{15}N-, ^{13}C, and 85% ^{2}H-labeled protein samples.

Sidechain aliphatic and aromatic resonances were assigned using a combination of ^{15}N-edited TOCSY, ^{15}N-edited NOESY, ^{13}C-edited NOESYs for methyl and aromatic groups. The $^{1}H^{\alpha}$ resonances were assigned using ^{15}N-edited TOCSY with 50 msec of DIPSI-II mixing. The TOCSY transfer was efficient enough to only reach the alpha protons. Other intra-residue aliphatic proton resonances were assigned using a combination of NOESYs including ^{15}N-edited NOESY (60 ms) and ^{13}C-edited NOESY (100 ms). The use of short-mixing time NOESYs for sidechain assignment was possible because both TM and cytoplasmic domains are almost completely helical, and thus inter-strand NOEs involving backbone amide and aliphatic protons are much weaker than the intra-residue NOEs. To further resolve the highly overlapped methyl proton resonances of BM2(26-109) in the carbon dimension and confirm their assignments, we recorded a 3D ^{1}H-^{13}C HMQC-NOESY-HSQC spectrum (100 ms NOE mixing, at 600 MHz) in which the t_1, t_2, and t_3 dimensions were ^{13}C, ^{13}C, and ^{1}H frequency labeled, respectively. The strong intra-residue NOEs between two methyl groups of valines and leucines were used to confirm methyl assignments in the more resolved carbon dimension. Specific stereo assignment of the methyl groups of valines and leucines were obtained from ^{1}H-^{13}C HSQC spectra (recorded with 28 msec constant-time ^{13}C evolution) of 15% ^{13}C-labeled protein samples [8].

The amide-methyl and methyl-methyl NOESY spectra of ILV-labeled BM2(26-109)

In addition to the conventional 3D ^{15}N-edited and ^{13}C-edited NOESYs used for assigning long range NOEs, we performed selective HN-Met and Met-Met NOESY experiments using an ILV-labeled BM2(26-109) sample. In this sample, the methyl groups of valines and leucines, and δ_1 methyl groups of isoleucines are ^{1}H-, ^{13}C-labeled and other aliphatic and aromatic positions are deuterated [9]. This labeling scheme removes the one-bond ^{13}C-^{13}C couplings and thus permits non-constant-time (non-CT) carbon evolution. The protein was reconstituted with deuterated LMPG detergent to prevent NOE dilution during NOE mixing. Two experiments were recorded and used for assigning both methyl resonances and inter-subunit NOEs. One experiment is a 3D version of the 4D (^{1}H-^{13}C HMQC)-NOESY-(^{1}H-^{13}C HSQC) experiment, with ^{13}C, ^{13}C, and ^{1}H evolution in the t_1, t_2, and t_3 dimensions, respectively. This spectrum was recorded at 600 MHz with NOE mixing time of 250 msec was used to assign inter-helical methyl-

methyl NOEs. Another experiment is a 3D (^{1}H-^{13}C HMQC)-NOESY-(^{1}H-^{15}N TROSY), in which the t_1, t_2, and t_3 dimensions are ^{13}C, ^{15}N, and ^{1}H frequency labeled, respectively. This experiment was recorded at 900 MHz with NOE mixing time of 300 msec. This experiment measures exclusively NOEs between backbone HN and sidechain methyl groups.

RDC measurement

For RDC measurement, the G-tetrad DNA liquid crystal [10] was used to weakly align BM2(26-109) in the presence of LMPG detergent. The reconstituted BM2(26-109) tetramer was dialysized against 50mM potassium phosphate, 50 mM KCl, pH 7.2 and concentrated in a centricon to a 140 ul solution with final protein concentration of 1 mM protein (monomer). A stock solution of dGpdG, made by dissolving 8 mg of dGpdG (Rasayan Inc.) in 140 ul H_2O, was first loaded to a Shigemi NMR tube before mixing with the protein solution. The 140 ul protein solution was then added to the NMR tube, followed by gentle mixing to allow formation of the G-tetrad DNA liquid crystal. The final aligned sample contains 0.5 mM protein (monomer), 200 mM LMPG, 25 mM Tris (pH 6.8), 100 mM KCl, and 5% D_2O. In a 600 MHz spectrometer, a quadrupolar coupling of 21 Hz was observed for D_2O in the aligned sample. The ^{1}H-^{15}N couplings were measured at 600 MHz (^{1}H frequency) using the *J*-scaled TROSY-HNCO experiment to fully exploit the favorable relaxation property of the TROSY transitions [11]. In this experiment, two 3D inter-leaved spectra were recorded, the regular TROSY-HNCO and a modified TROSY-HNCO with NH coupling scaled to bring the TROSY peak up to the decoupled position. RDCs were extracted by subtracting *J* couplings acquired with the regular sample from the $J + D$ couplings of the weakly aligned sample.

Nature Structural & Molecular Biology: doi:10.1038/nsmb.1707

Supplementary Figures

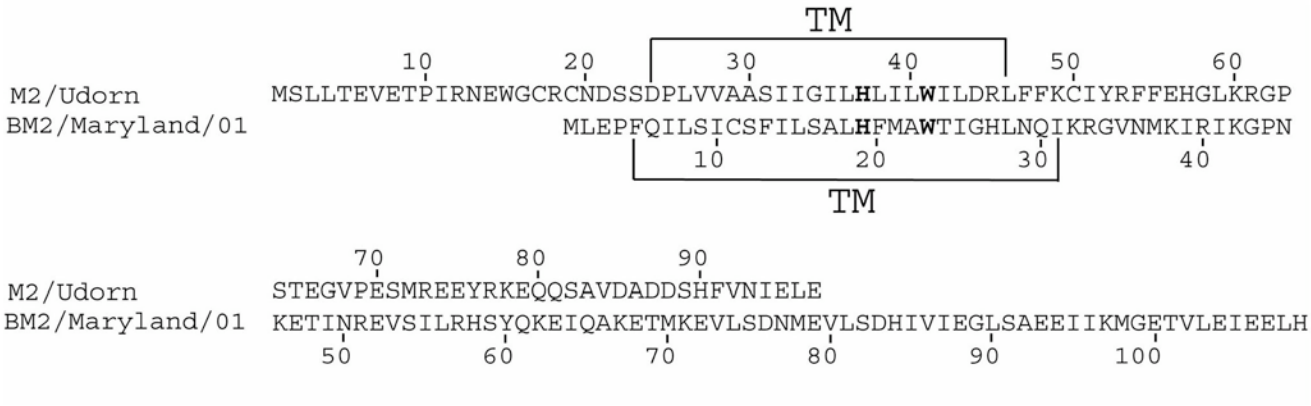

Supplementary Figure 1. Amino acid sequences of AM2 (Udorn) and BM2 (Maryland/01), aligned at the HXXXW motif in the TM domain. In this study, Cys11 is replaced with serine to simplify purification.

Nature Structural & Molecular Biology: doi:10.1038/nsmb.1707

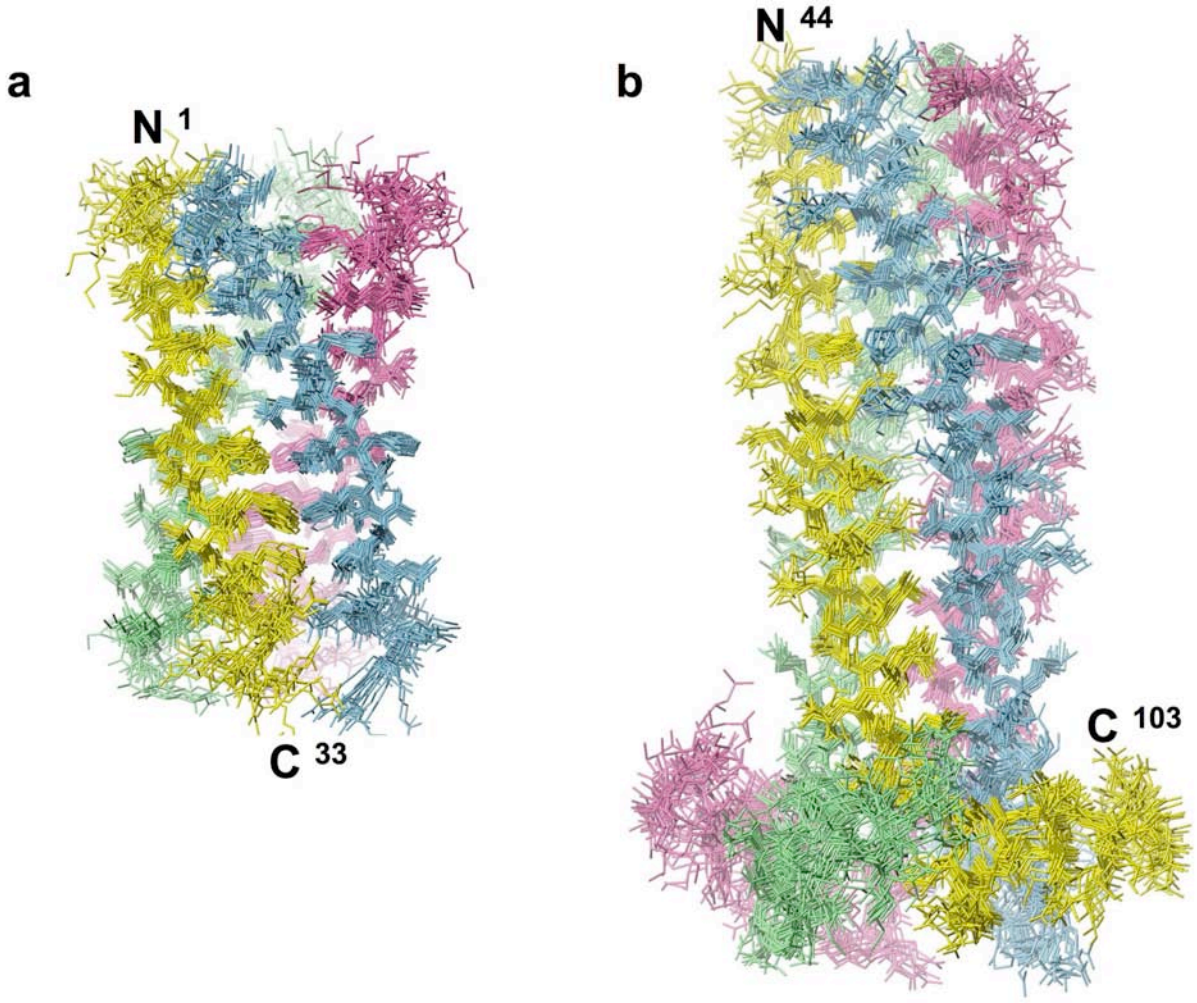

Supplementary Figure 2. Structural ensembles. **a,** An ensemble of 15 low-energy structures derived from NMR restraints from the BM2(1-33) construct. The structures are superimposed on all heavy atoms from residues 4 – 32. The r.m.s. deviations for backbone and all heavy atoms are 0.70 Å and 1.06 Å, respectively. **b,** An ensemble of 15 low-energy structures derived from NMR restraints from the BM2(26-109) construct. The structures are superimposed on all heavy atoms from residues 44 – 103. The r.m.s. deviations for backbone and all heavy atoms are 0.92 Å and 1.38 Å, respectively.

Nature Structural & Molecular Biology: doi:10.1038/nsmb.1707

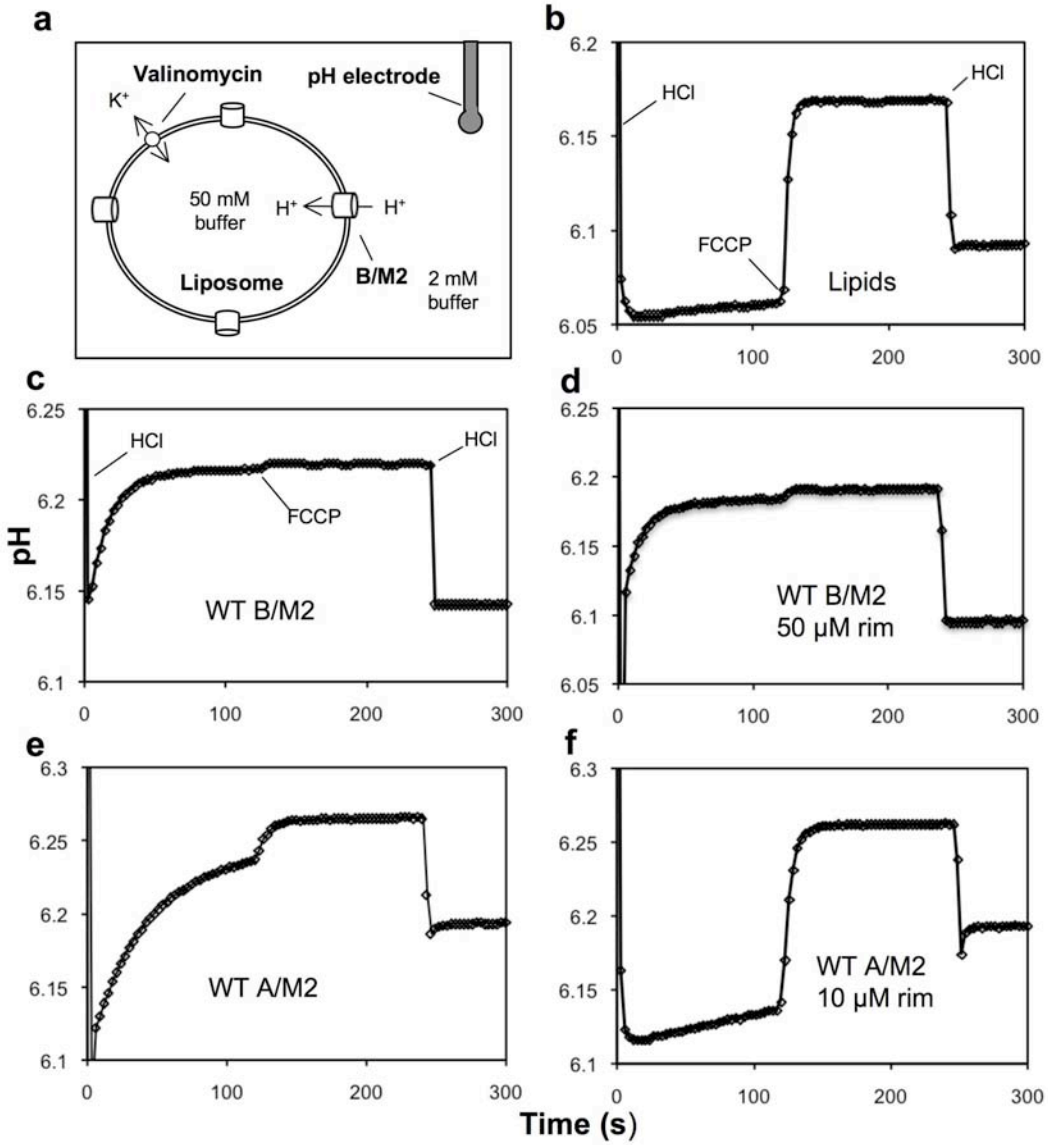

Supplementary Figure 3. The liposomal proton flux assay. **a,** Schematic illustration of the BM2 activity assay set-up. **b,** Proton permeability of the membrane is minimal in the absence of proteins. **c,** Proton flux assay for 1.5 M of WT BM2(1-33). The assay was initiated by the addition of protons (as HCl) to the external solution. BM2(1-33) channel activity results in recovery of the pH as protons are conducted into the liposome interior. The experiment was terminated by addition of the proton uncoupler FCCP. The buffering capacity of the system is then measured by adding a known quantity of protons. The same assay was performed for BM2(1-33) in the presence of 50 M rimantadine **(d)**, 3 M of WT AM2(18-60) **(e)**, and WT AM2(18-60) in the presence of 10 M rimantadine **(f)**.

Nature Structural & Molecular Biology: doi:10.1038/nsmb.1707

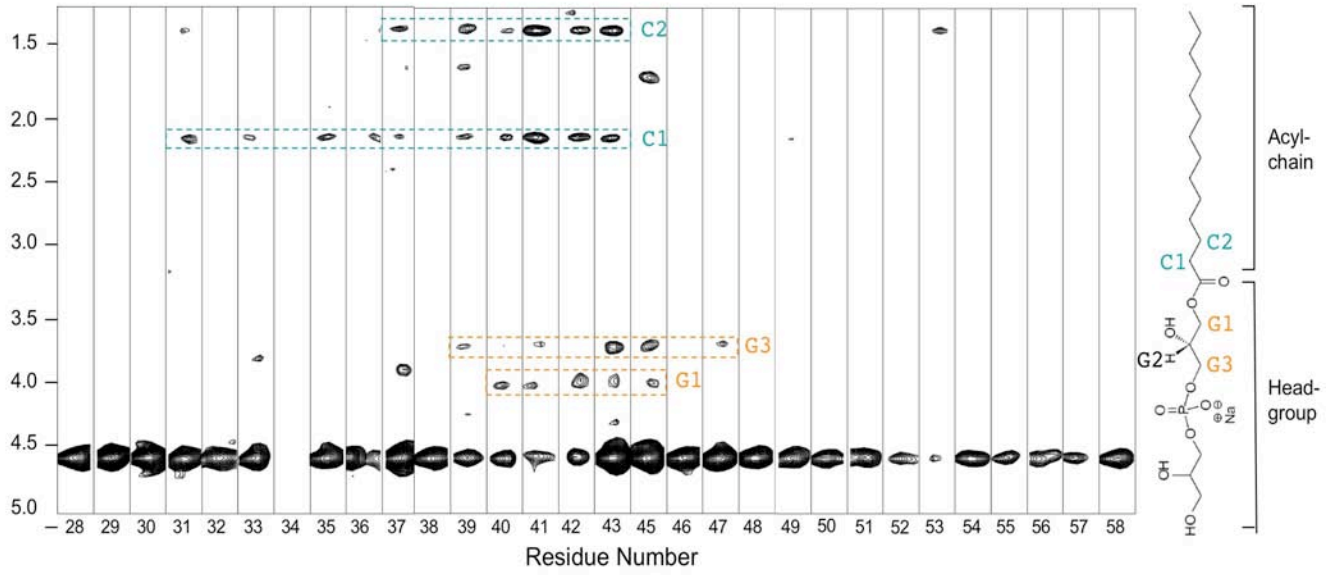

Supplementary Figure 4. 3D ^{15}N-edited NOESY spectrum recorded with NOE mixing time of 300 ms at ^{1}H frequency of 600 MHz on a sample containing ^{15}N-, ^{2}H-labeled BM2(26-109) and LMPG detergent. NOEs between amide protons of BM2(26-109) and head group protons (G1 and G3) of LMPG detergent were interpreted qualitatively as atom-to-plane restraints in modeling the full-length BM2 relative to the presumed lipid bilayer.

Nature Structural & Molecular Biology: doi:10.1038/nsmb.1707

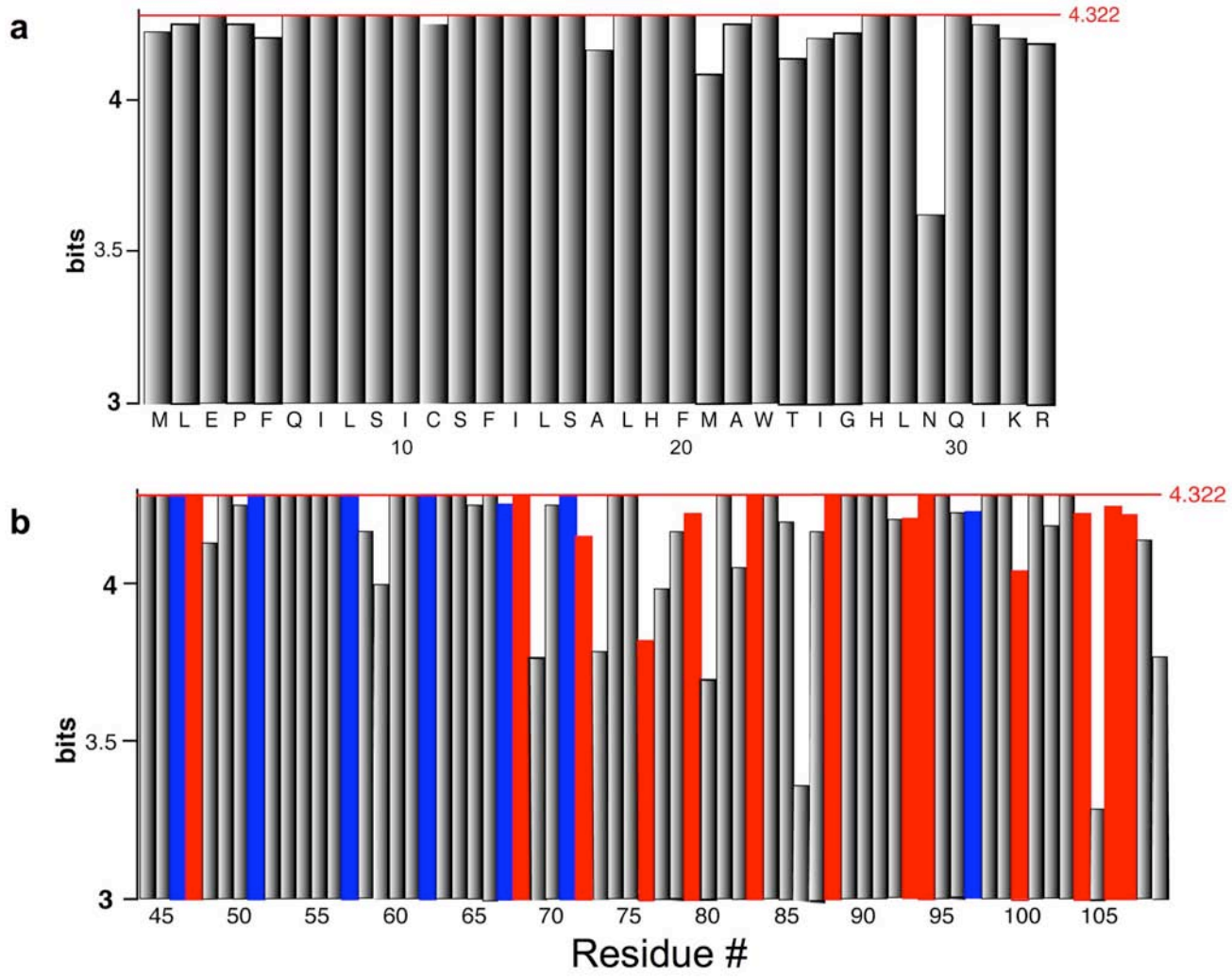

Supplementary Figure 5. Sequence conservation of the TM domain **(a)** and the cytoplasmic domain **(b)** of BM2. The red horizontal line at bits value of 4.322 marks 100% conservation. In **(b)**, the bars corresponding to the positively and negatively charged residues on the protein surface are colored in blue and red, respectively. The sequences were downloaded from NCBI Influenza Virus Resource (http://www.ncbi.nlm.nih.gov/genomes/FLU/FLU.html). The conservation calculated was performed with the weblogo server (http://weblogo.berkeley.edu).

Nature Structural & Molecular Biology: doi:10.1038/nsmb.1707

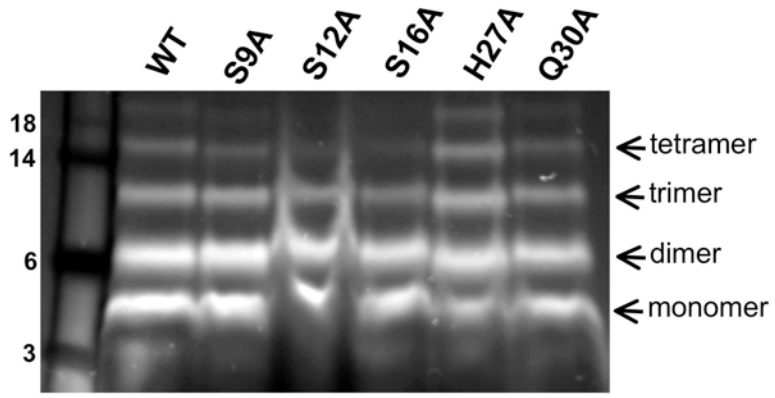

Supplementary Figure 6. Chemical crosslinking of BM2(1-33) and its variants. SDS-PAGE of BM2(1-33) variants after being treated with 50 M DSP for 15 min.

Nature Structural & Molecular Biology: doi:10.1038/nsmb.1707

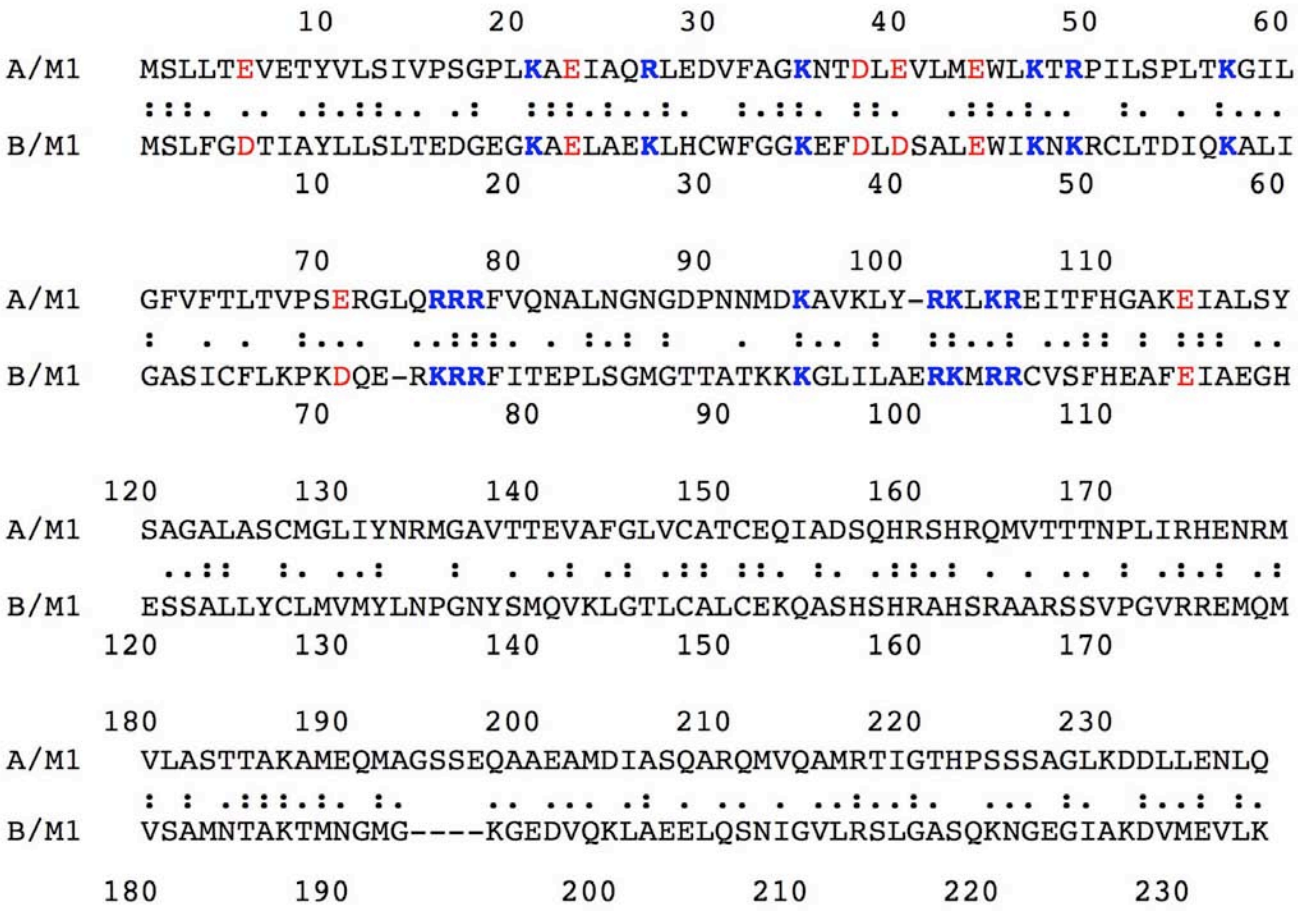

Supplementary Figure 7. Sequence alignment of AM1 and BM1 shows 30% identity between the two proteins. Based on the crystal structure of AM1(1-158) (PDB code: 1aa7), the surface charged residues are colored in blue and red for the positively charged and negatively charged amino acids, respectively.

Nature Structural & Molecular Biology: doi:10.1038/nsmb.1707

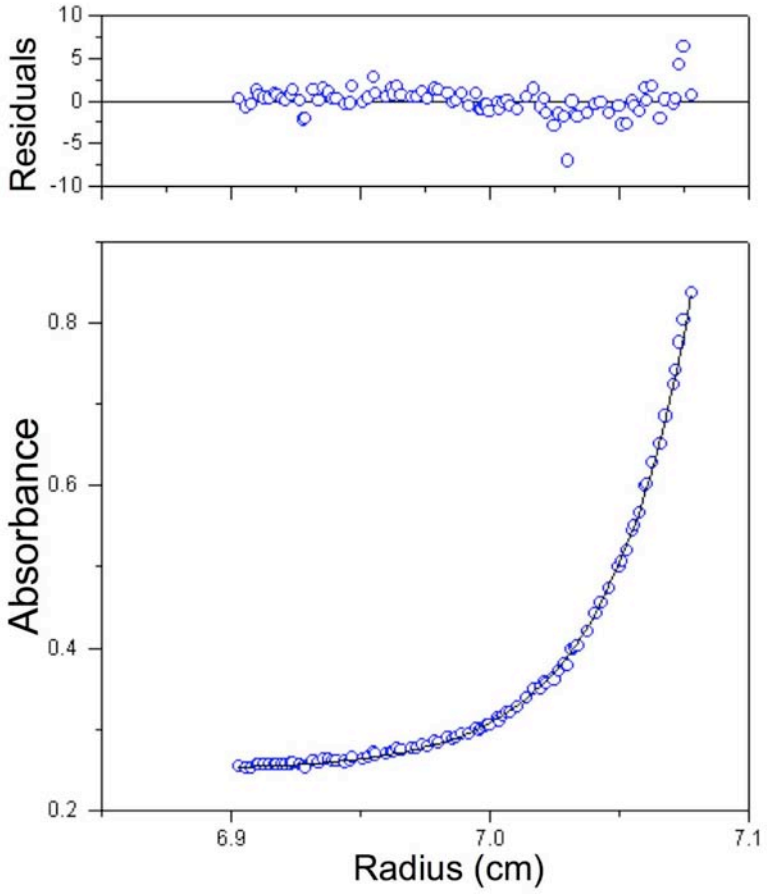

Supplementary Figure 8. Analytical ultracentrifugation (AUC) analysis of the water-soluble BM2(43-109). A molecular weight (MW) of 35.7 kDa was derived from AUC curve fittings from 9 measurements with 3 different concentration (0.5 mM, 0.25 mM and 0.125 mM) and 3 centrifugation speeds (20 k, 30 k and 40 k). Comparing to a monomer M.W. of 8.5 kDa, AUC measurements shows that BM2 (43-109) forms homogeneous tetramers in water.

Nature Structural & Molecular Biology: doi:10.1038/nsmb.1707

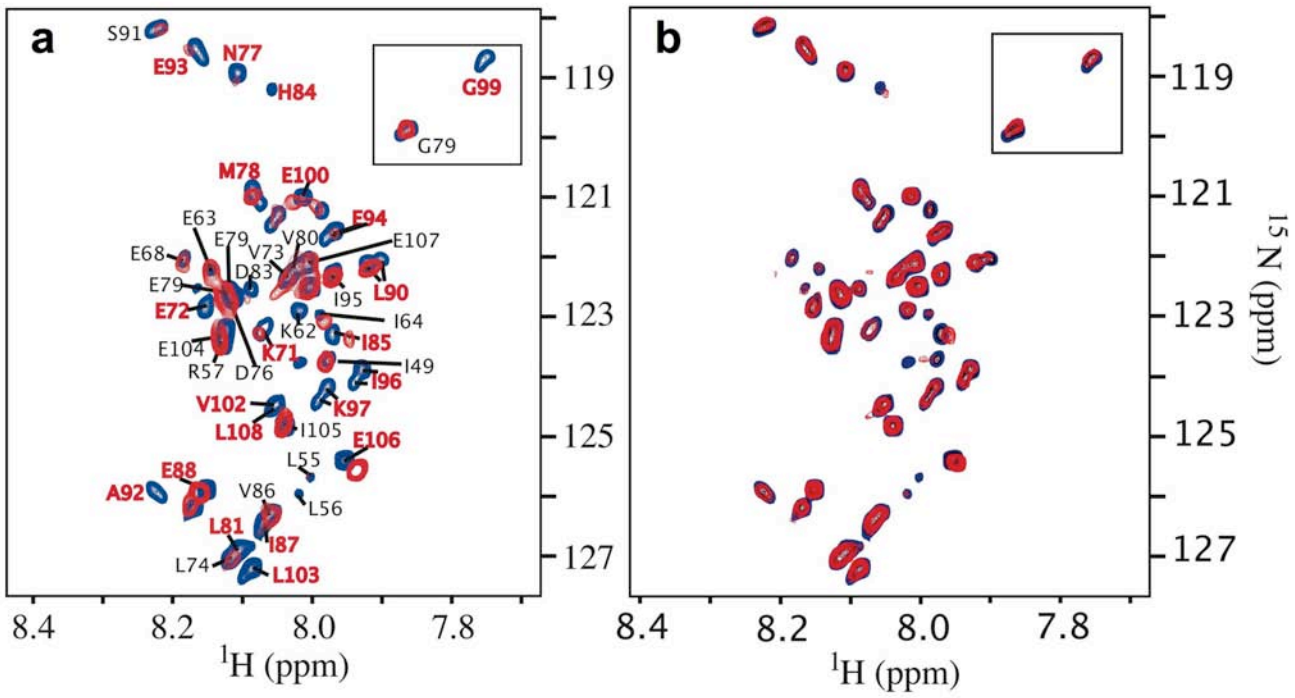

Supplementary Figure 9. Perturbation of BM2(43-109) chemical shift by the binding of MBP-BM1. **a,** Overlay of ^{1}H-^{15}N TROSY spectra of BM2(43-109) in the absence (blue) and presence (red) of MBP-BM1. The labeled resonances are those whose assignments could be correctly traced. **b,** The negative control; spectra of BM2(43-109) in the absence (blue) and presence (red) of MBP.

Nature Structural & Molecular Biology: doi:10.1038/nsmb.1707

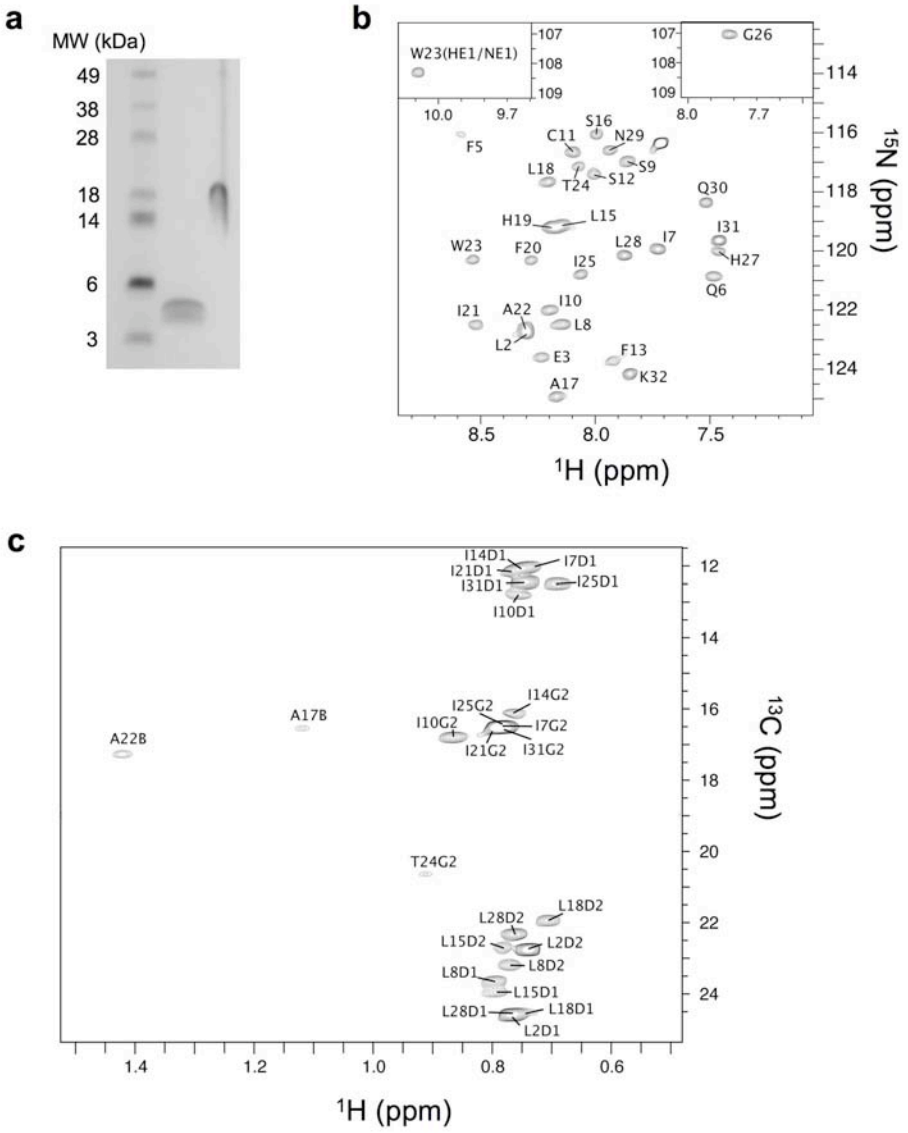

Supplementary Figure 10. Biochemical and NMR characterization of BM2(1-33) tetramer reconstituted in DHPC micelles. **a,** SDS-PAGE of BM2(1-33). Lane 1: not boiled and not reconstituted; lane 2: not boiled and reconstituted in DHPC. **b,** ^{1}H-^{15}N TROSY (recorded at ^{1}H frequency of 600 MHz) of ^{15}N-, ^{2}H-labeled and reconstituted BM2(1-33) at pH 7.5. **c,** ^{1}H-^{13}C HSQC spectrum of reconstituted BM2 (1-33), showing the assignments of methyl resonances.

Nature Structural & Molecular Biology: doi:10.1038/nsmb.1707

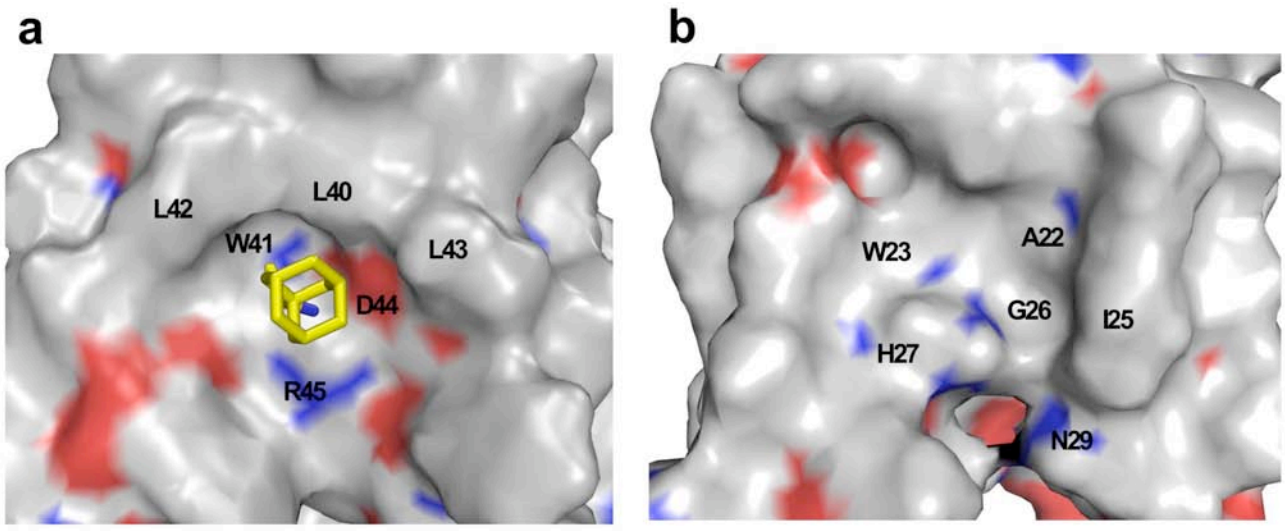

Supplementary Figure 11. BM2 does not have the rimantadine binding site observed in AM2. **a,** The surface representation of the rimantadine-binding pocket in AM2 [13]. The adamantane group of rimantadine is colored in yellow and the amino group is colored in blue. **b,** The surface representation of the corresponding region of the channel in BM2.

Nature Structural & Molecular Biology: doi:10.1038/nsmb.1707

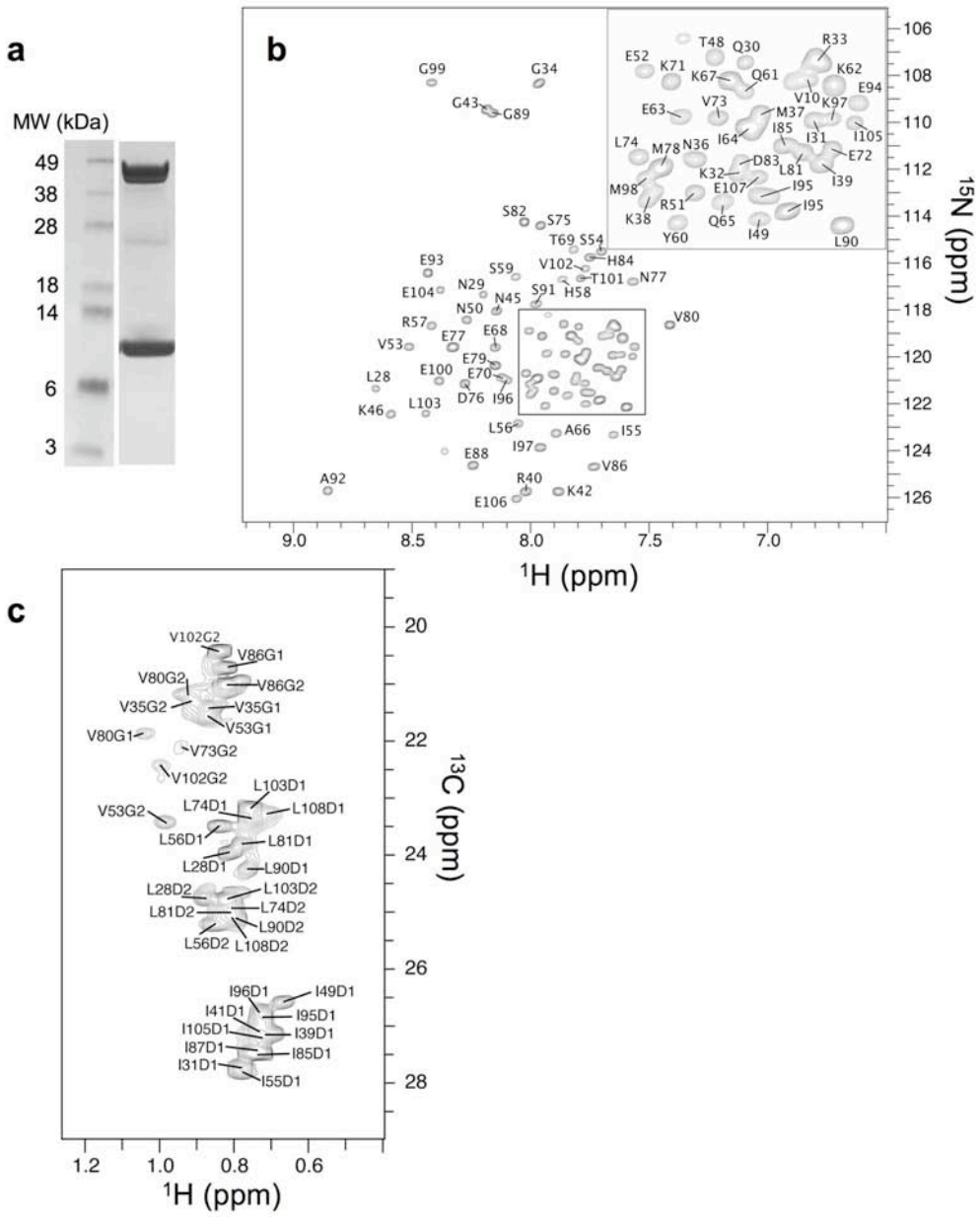

Supplementary Figure 12. Biochemical and NMR characterization of BM2(26-109) tetramer bound to LMPG micelles. **a,** SDS-PAGE of BM2(26-109) in the presence of LMPG micelles (not boiled). **b,** ^{1}H-^{15}N TROSY (recorded at ^{1}H frequency of 600 MHz) of ^{15}N-, ^{2}H-labeled and reconstituted BM2(26-109) at pH 6.8. **c,** ^{1}H-^{13}C HSQC spectrum of reconstituted BM2 (26-109) (ILV labeled), showing the assignments of methyl resonances. The isoleucine δ1 resonances are folded in the ^{13}C dimension.

Nature Structural & Molecular Biology: doi:10.1038/nsmb.1707

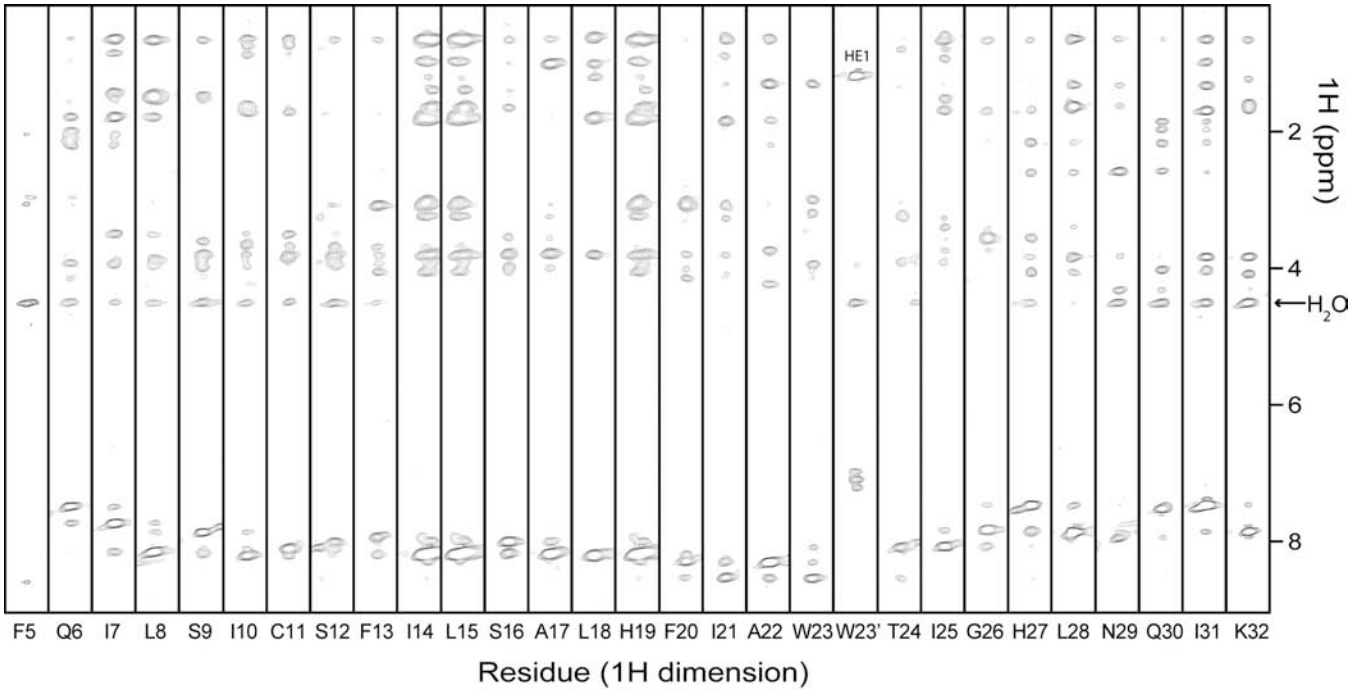

Supplementary Figure 13. ^{15}N-edited NOESY of BM2(1-33). The ^{1}H-^{15}N strips corresponding to residues 5 – 32 from the 3D ^{15}N-edited NOESY with water-gate readout pulse scheme, recorded at ^{1}H frequency of 600 MHz on a sample containing 1 mM protein (monomer), 300 mM D35-DHPC, 40 mM sodium phosphate (pH 7.5) and 30 mM glutamate. The spectrum was acquired with 110 ms NOE mixing time, 36 ms of ^{15}N evolution and 19 ms ^{1}H evolution in the indirect dimension.

Nature Structural & Molecular Biology: doi:10.1038/nsmb.1707

Supplemental References

1. Delaglio, F. et al. NMRPipe: a multidimensional spectral processing system based on UNIX pipes. J. Biomol. NMR 6, 277-293 (1995).
2. Keller, R. (2004).
3. Cornilescu, G., Delaglio, F. & Bax, A. Protein backbone angle restraints from searching a database for chemical shift and sequence homology. J. Biomol. NMR 13, 289-302 (1999).
4. Losonczi, J. A., Andrec, M., Fischer, M. W. F. & Prestegard, J. H. Order matrix analysis of residual dipolar couplings using singular value decomposition. J. Magn. Reson. 138, 334-342 (1999).
5. Zweckstetter, M. & Bax, A. Prediction of sterically induced alignment in a dilute liquid crystalline phase: aid to protein structure determination by NMR. J. Am. Chem. Soc. 122, 3791-3792 (2000).
6. Salzmann, M., Wider, G., Pervushin, K. & Wuthrich, K. Improved sensitivity and coherence selection for [N-15,H-1]-TROSY elements in triple resonance experiments. J. Biomol. NMR 15, 181-184 (1999).
7. Kay, L. E., Ikura, M., Tschudin, R., Bax, A. Three-dimensional triple resonance NMR spectroscopy of isotopically enriched proteins. J. Magn. Reson. 89, 496-514 (1990).
8. Szyperski, T., Neri, D., Leiting, B., Otting, G. & Wuthrich, K. Support of 1H NMR assignments in proteins by biosynthetically directed fractional 13C-labeling. J. Biomol. NMR 2, 323-334 (1992).
9. Tugarinov, V., Kanelis, V. & Kay, L. E. Isotope labeling strategies for the study of high-molecular-weight proteins by solution NMR spectroscopy. Nat Protoc 1, 749-54 (2006).
10. Lorieau, J., Yao, L. & Bax, A. Liquid Crystalline Phase of G-Tetrad DNA for NMR Study of Detergent-Solubilized Proteins. J. Am. Chem. Soc. 130, 7536-7 (2008).
11. Kontaxis, G., Clore, G. & Bax, A. Evaluation of cross-correlation effects and measurement of one-bond couplings in proteins with short transverse relaxation times. J. Magn. Reson. 143, 184-196 (2000).
12. Laskowski, R. A., MacArthur, M. W., Moss, D. S. & Thornton, J. W. PROCHECK: a program to check the stereochemical quality of protein structures. J. Appl. Cryst. 26, 283-291 (1993).
13. Schnell, J. R. & Chou, J. J. Structure and mechanism of the M2 proton channel of influenza A virus. Nature 451, 591-5 (2008).

Nature Structural & Molecular Biology: doi:10.1038/nsmb.1707